JOURNAL OF MATERIALS SCIENCE **34** (1999) 4439–4445

Effect of BaO and SiO_2 addition on PTCR $BaTiO_3$ ceramics

GAOSHENG LIU, R. D. ROSEMAN
Department of Materials Science and Engineering, University of Cincinnati, Cincinnati, OH 45221-0012, USA
E-mail: gaosheng.liu@tod.com

The influence of Ba-excess and liquid phase sintering with SiO_2 on the electrical conduction and microstructure in PTCR $BaTiO_3$ has been investigated. Dense (95–96%), small grain (5–10 μm) PTCR materials were obtained in Ba-excess (Ba/Ti = 1.006) $BaTiO_3$. The materials exhibit low room temperature resistivity ρ_{RT} (10^0–10^2 Ω·cm) and high PTCR respond (more than 5 orders). Solid state sintering was found to inhabit the semiconducting and PTCR behavior in Ba-excess materials. Liquid phase sintering, using SiO_2 in the Ba-excess $BaTiO_3$, resulted in low ρ_{RT} and significant PTCR response. Through domain observation, interior "Polaron deficient zones" were found in samples which exhibit limited liquid phase sintering, leading to non-uniform directional domains and low charge carrier mobility. Proper control of the SiO_2 concentration was found critical for obtaining uniform directional domain microstructures and low ρ_{RT}.

1. Introduction

The PTCR effect of $BaTiO_3$ is that a nonlinear resistivity change near the Curie Point due to a mixed electrical conduction effect of spontaneous polarization and semiconducting behavior of a doped ferroelectric polycrystalline [1–3]. Semiconducting $BaTiO_3$ ceramics with low room temperature resistivity (ρ_{RT}) and high PTCR effect performance is attractive to fabricate in order to meet various demand in many electronic devices [3]. Both ρ_{RT} and PTCR response depends on composition (donor and acceptor doping as well as stoichiometry) and processing parameters, especially heat treatment schedules. During sintering, the interaction between the various dopants (donor Y^{3+}, La^{3+} or acceptor Mn^{3+} ions etc.) and excess TiO_2 or BaO creates the chemical defects and modifies the stress distribution [4, 5]. This activates the electrical and mechanical compensating mechanism, especially within near grain boundary regions [6]. The defects, along with the ferroelectric spontaneous polarization and domain structure will dominate the nature of grain and grain boundary and determine the electron transportation processes [7].

SiO_2 and excess TiO_2 are usually added in order to create a liquid phase and reduce sintering temperature [8]. The eutectic temperature of Ti-excess is around 1320 °C. After addition of SiO_2, this temperature decreases to approximately 1260 °C [9]. The dispersion of dopants in the material and microstructure uniformity can be promoted by the presence of SiO_2. In $BaTiO_3$ system with small excess of TiO_2 and SiO_2, Ueoka clarified the existence of at lease two phases in the grain boundary in the specimens, $BaTi_3O_7$, and a glassy phase assumed to be $BaTiSiO_5$ [10]. In a wide concentration range of titanium-rich liquid phase, ρ_{RT} was found to be roughly constant, and the intensity of the PTCR effect to be dependent on the amount of second phase [2]. Udayakumar studied Ba-excess $BaTiO_3$ ceramics with the Ba/Ti ratio = 1.02 doped with Nb and Si. The samples showed a very low ρ_{RT} and exhibited a resistivity jump at the Curie point [8].

Electrical conduction in materials depends on the concentration of charge carriers and their mobility in polycrystalline materials. A polaron model associated with Ti-site is usually used to explain the electrical conduction in n-type $BaTiO_3$ grain [4]. The most acceptable PTCR model of $BaTiO_3$ is the grain boundary electrical barrier model, which first was established by Heywang, then refined below the Curie point by Jonker [11–14]. Subsequent studies focused on refining the models with respect to grain boundary barrier layers and defect chemistry [15–18]. In the semiconducting $BaTiO_3$, determination of the various defects is very complex and most techniques can not measure due to the low concentration of dopants. Possible defects include vacancies of Barium, Titanium and oxygen ions along with the dopant occupied sites [2, 19]. These defects locate within grains or segregate at grain boundaries. The kinetic behavior of defects depends on dopant concentration, sintering and annealing schedule. A model in which the electrical potential barrier is established by Ba vacancies was developed by Danials and a "Ti vacancy" model was proposed by Lewis [15, 20, 21]. Yet neither was able to fully explain the experimental results as a function of stoichiometry (Ba/Ti ratio) very well.

Ba-excess $BaTiO_3$ ceramics have much lower concentration of oxygen vacancies than that of Ti-excess, which was confirmed through as aging studies [22, 23].

PTCR $BaTiO_3$ ceramics with higher proportion of Ba, therefore, was given attention for both application and theoretical understanding of PTCR ceramics although it is difficult to obtain the semiconducting behavior by the addition of extra BaO [9, 19]. The interplay between extra BaO and various dopants determines the secondary phase and defect distribution, as well as domain formation. The present paper focuses on studying the sintering behavior and electrical properties of doped $BaTiO_3$ as a function of the BaO and addition of liquid phase. Domain orientation pattern in $BaTiO_3$ with addition of BaO and SiO_2 are also investigated with some detail.

2. Experimental

The ceramics were prepared by typical wet milling methods. $BaTiO_3$ with a variety of ratio Ba/Ti = 0.997, 1.000, 1.003 were selected as raw materials. $BaTiO_3$ with Ba/Ti = 1.006 can be obtained by adding barium acetate to $BaTiO_3$ powder with ratio Ba/Ti = 1.003. The dopants, Y_2O_3, or La_2O_3 were added as nitrate solution [18]. The batches were divided into two groups. In the first group, $BaTiO_3$ with various Ba/Ti ratios were doped with same amount of Y_2O_3 or La_2O_3. In the second group, Ba-excess $BaTiO_3$ with Ba/Ti = 1.006 was doped with (1) $Y_2O_3 + 2$ mol % SiO_2, and (2) $Y_2O_3 + 0.07\%$ MnO + 2 mol % SiO_2.

The liquid media used was deionized water and isopropyl alcohol in wet milling. PVA, carbowax together with fish oil mixture for the binder, lubricant and deflocculant purpose. After ball milling, the solution was dried by a lab scale spray dryer and resultant powders were pressing into 12 mm diameter and 2 mm thickness discs. Heat treatment consists of a fixed heating rate with various sintering temperatures, a constant cooling rate with different annealing period with annealing temperature 1220 °C.

Resistivity as a function of temperature was measured using a dc power supply (0.015 V) and Keithley 614 electronmeter as a picoammeter. The microstructure of as-sintered surfaces and acid etched surfaces were taken by SEM in order to obtain the features of grain and domain structure. The average grain size was also determined by the linear intercept technique.

3. Results and discussion

3.1. Ba-excess effect

The densification of PTCR $BaTiO_3$ ceramics near a narrow region around the ratio (Ba/Ti = 1.000) strongly depend on the deviation of the ratio of Ba/Ti [5]. Fig. 1 shows the as-sintered surfaces of (0.18 mol % Y_2O_3) modified $BaTiO_3$ with different Ba/Ti at sintering temperature 1350 °C. The average grain size reduces from 30 μm in $BaTiO_3$ with Ba/Ti = 0.997 samples to 1 μm in $BaTiO_3$ with Ba/Ti = 1.006, illustrating a transition of typical liquid phase to solid state sintering. For $BaTiO_3$ ceramic with Ba/Ti = 1.006, it was thought that the secondary phase Ba_2TiO_4 and absence of liquid phase inhibit the grain growth [5]. The dependence of densification behavior on the Ba/Ti ratio is shown in Fig. 2. With a Ba/Ti ratio ≤1.003, the results indicate a typical liquid phase sintering trend with increasing sintering temperature. The eutectic temperature is 1320 °C, in accordance with the temperature of the Ti-excess side indicated in the BaO-TiO_2 phase diagram [24].

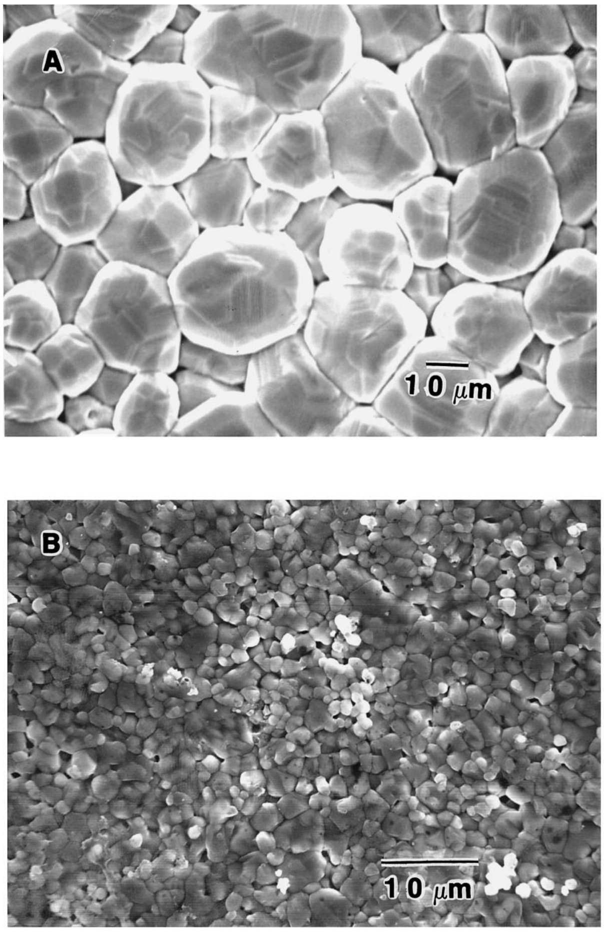

Figure 1 SEM microscope of sintered surface for (A) Ba/Ti = 0.997 and (B) Ba/Ti = 1.006.

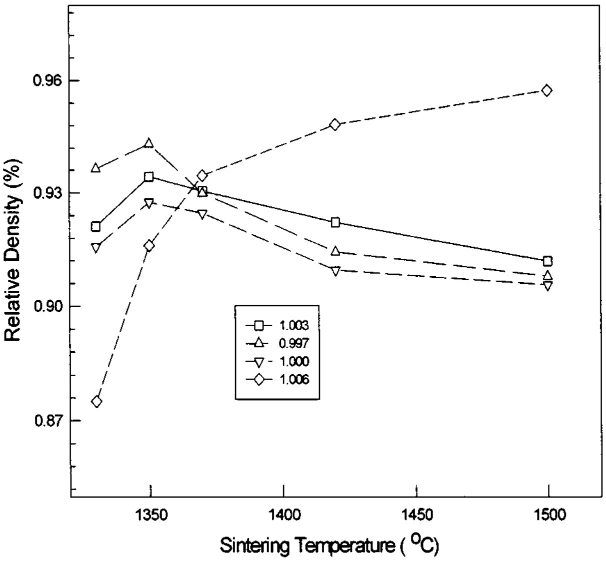

Figure 2 Relative density as a function of Ba/Ti ratios and the sintering temperatures.

The density increases within increasing sintering temperature until 1350 °C, followed by a decrease in

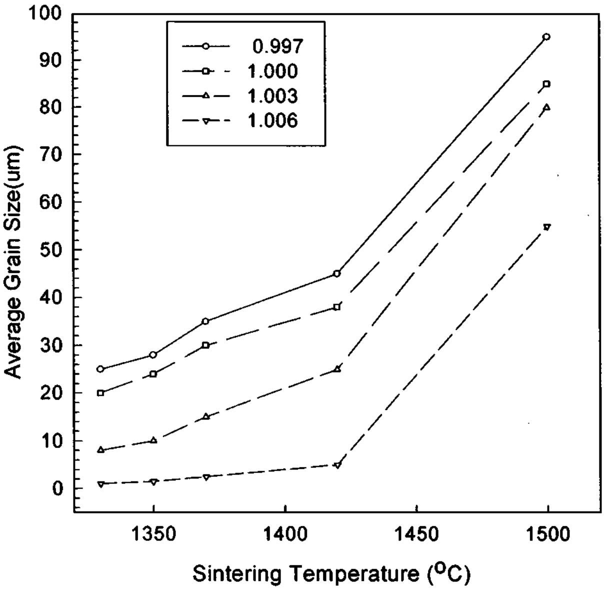

Figure 3 Average grain size as a function of Ba/Ti ratios and the sintering temperatures.

density with increasing sintering temperature. When the Ba/Ti ratio reaches 1.006, a different trend is found and the material exhibits solid state sintering below 1420 °C, above which a eutectic reaction occurs as observed by the samples sintered surface. Even though the eutectic temperature on Ba-excess side of the phase diagram is approximately 1560 °C [24], this temperature is greatly lowered due to the added dopants and only a small Ba-excess concentration, which is not well defined within this region in the phase diagram. The maximum density for Ba-excess $BaTiO_3$ is approximately 96% as the sintering temperature increases to 1500 °C. Fig. 3 shows the average grain size with Ba/Ti ratio. A small grain size (1–5 μm) was obtained in Ba-excess $BaTiO_3$ within the sintering temperature range of 1320–1420 °C. The material with optimum density (95%) and 5 μm grain size was obtained by sintering at 1420 °C. Figs 2 and 3 demonstrate that the eutectic temperature associated with densification and grain growth behavior in $BaTiO_3$ systems with a Ba/Ti ratio < 1.006 is similar to typical Ti-excess systems. Hence, Ba-excess $BaTiO_3$ character can be identified with a Ba/Ti ratio of ≥ 1.006 as samples were prepared from the same lot of powders. In this paper, Ba-excess $BaTiO_3$ referring to materials with the Ba/Ti ratio $= 1.006$ is mostly concerned.

Fig. 4 shows resistivity vs. temperature behavior in doped $BaTiO_3$ as function of Ba/Ti ratio and a sintering temperature of 1350 °C. Samples with a Ba/Ti ≤ 1.003 have dark blue color, indicating the presence of Ti^{3+} [2]. A low ρ_{RT} (10^1–10^4 Ω·cm) with significant magnitude of PTCR rise is obtained. With a Ba/Ti ratio of 1.0045, a moderately high ρ_{RT} (10^5–10^6 Ω·cm) with a shallow PTCR rise (0.5–1 order) was obtained. As the ratio increases to 1.006, the room temperature resistivity greatly increases (10^{11} Ω·cm) and the PTCR anomaly no longer exists. The samples are yellow in color, illustrating that limited reduction compensation by Ti^{3+} exists. These materials exhibit typical insulating behavior. The insulating properties in Ba-excess $BaTiO_3$ are caused by the fact that only a limited amount of liquid phase is generated below 1420 °C and it is not sufficient to disperse Y_2O_3 properly for uniform donor diffusion. Higher sintering temperatures were, therefore, needed to generate a liquid phase in Ba-excess samples. It was found, though, that insulating behavior exists even though the sintering temperature was in the range of 1420–1500 °C. Possible mechanisms for the insulating behavior are given below.

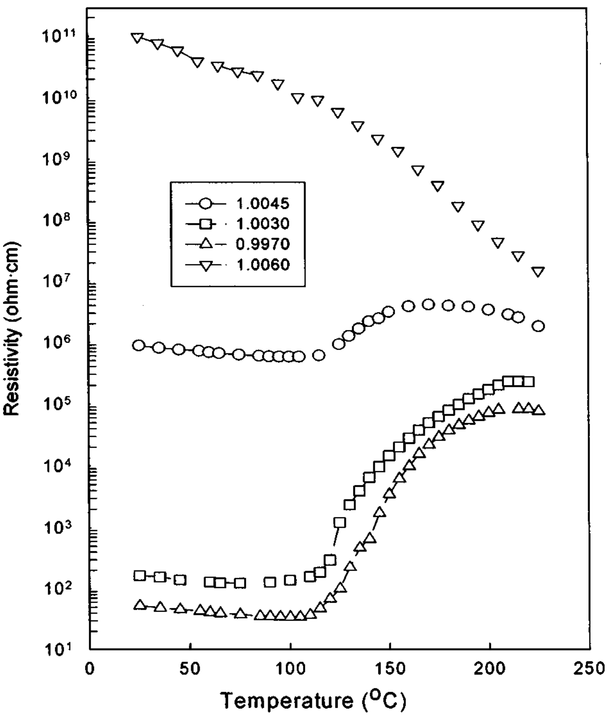

Figure 4 PTCR behavior in donor doped $BaTiO_3$ with different Ba/Ti ratio.

(1) *Y^{3+} Self-Compensation*. Insulating behavior stems from Y^{3+} substituting on both cation sites due to its intermediate radius between Ba^{2+} and Ti^{4+}, which leads to a self-compensation [17]. To clarify the substitution questions, La_2O_3 was used in place of Y_2O_3 as the donor in Ba-excess $BaTiO_3$. The La^{3+} radius is close to that of Ba^{2+} [2]. La_2O_3 doping showed similar electrical behaviors in samples of various sintering schedules, illustrating insulating behavior is not dominated by Y_2O_3 self compensation. On the other hand, calculation of the solution formation energy by Lewis also shows a much higher preference of Y substitution to the Ba site than to the Ti site, which also denies the possibility of Y_2O_3 self-compensation [20, 21].

(2) *The Chemical Reaction between BaO and Y_2O_3*. There may exist a reaction between Y_2O_3 and excess BaO to form new components BaY_2O_4 and $Ba_3Y_4O_9$, which occurs at 1400 °C according to the BaO-Y_2O_3 phase diagram. Occurrence of this reaction limits the amount of remnant donor availability and the concentration becomes too low to create semiconducting behavior. Experimental results indicated that slightly increasing the donor concentration to from 0.18 to 0.3 mol % does not result in semiconducting behavior. It is also known that further increasing the Y_2O_3 concentration leads to cation vacancy compensation

and insulating behavior, leading a difficulty to distinguish the influence to electrical properties by this reaction [1, 3]. However, this mechanism should not be considered as the main reason for insulating behavior in Ba-excess materials as long as Y_2O_3 is well dispersed.

(3) *Formation of Ti Vacancy Layer*. At high sintering temperatures, Ba^{2+} diffusion leads to the concentration of Ti^{4+} vacancies increase greatly at grain surface layers and diffusing into the interior [15]. During cooling from sintering they become "frozen-in". As a consequence, the extra positive charges by $Y^{\cdot}_{Ba}$ are completely compensated by Ti^{4+} vacancies, instead of Ti^{4+} reduction to Ti^{3+}, to maintain neutrality. The bulk defect equation for sintering above 1420 °C can be written in Kroger-Vink form as Equation 1 [25]. This type of defect chemistry most realistically dominates the materials behavior, limiting semiconducting behavior.

$$2Y_2O_3 \xrightarrow{\text{Ba-excessBaTiO}_3} 4Y^{\cdot}_{Ba^{2+}} + V''''_{Ti^{4+}} + 6O_O \qquad (1)$$

3.2. Liquid phase sintering with SiO_2

The introduction of SiO_2 in Ba-excess $BaTiO_3$ creates a low temperature liquid phase and transfers the material back to one which exhibits low room temperature resistivity with PTCR behavior. The color of these samples is blue, indicating the presence of Ti^{3+}.

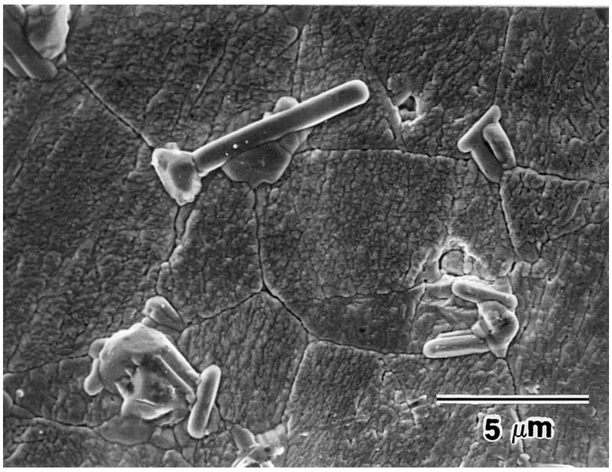

Figure 6A Thermal Etched surface of Ba-excess $BaTiO_3$ with SiO_2 addition.

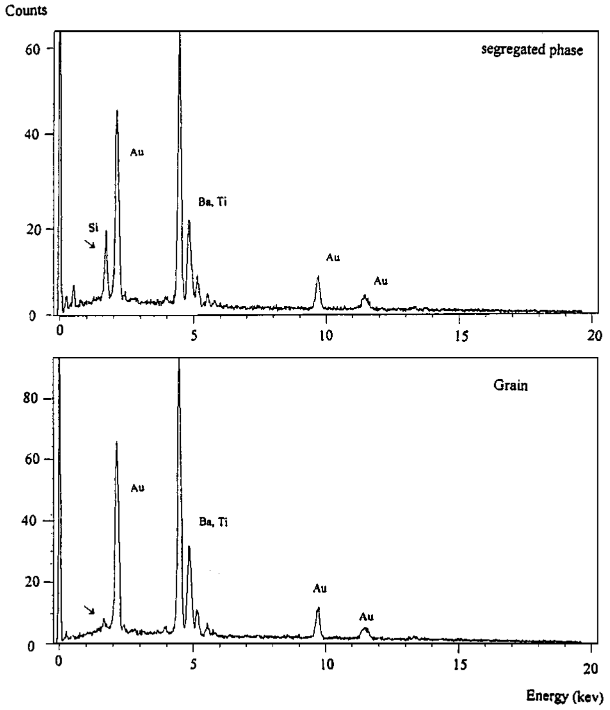

Figure 6B EDX spectrums of SiO_2 added Ba-excess $BaTiO_3$ corresponding to Fig. 6A.

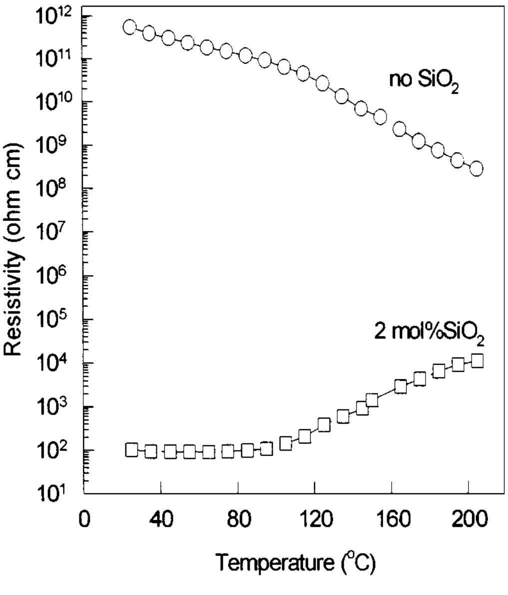

Figure 5 PTCR behavior in Ba-excess $BaTiO_3$ as a function of SiO_2 addition.

Fig. 5 shows the resistivity behavior of Ba-excess $BaTiO_3$ as a function of SiO_2. ρ_{RT} decreases 10 orders of magnitude. The phases containing the Si were found to mainly segregate at the grain boundary triple points, as shown in the SEM micrograph (Fig. 6A) of a thermally etched surface. EDX analysis of grains and segregated phases is shown in Fig. 6B. Si is barely detected within $BaTiO_3$ grains, illustrating that SiO_2 changes the defect structure not directly by its own diffusion and substitution, instead, it incorporates dopants during densification to improve dopant dispersion [6]. The defect equation for this reaction is given by Equation 2

$$Y_2O_3 \xrightarrow[\text{SiO}_2\text{addition}]{\text{Ba-excessBaTiO}_3} 2Y^{\cdot}_{Ba^{2+}} + 2Ti^{3+\prime}_{Ti^{4+}} + 3O_O \qquad (2)$$

Various SiO_2 concentrations were added to donor doped (Y_2O_3: 0.3 mol %) Ba-excess $BaTiO_3$ to determine optimum SiO_2 concentration. Fig. 7 shows the density and average grain size as a function of SiO_2 content at a sintering temperature of 1330 °C. As the concentration of SiO_2 increases, the relative density increase from 89–97% with a concentration 1 mol % of SiO_2. It slightly decreases to 95% with 2 mol % and further decreases to 87% with 3 mol % addition. These results show that a high-density material can be obtained

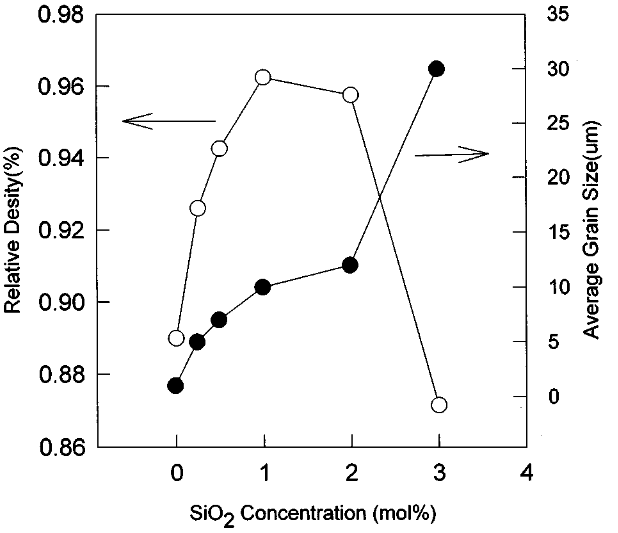

Figure 7 Density and average grain size in Ba-excess $BaTiO_3$ as a function of SiO_2 concentration.

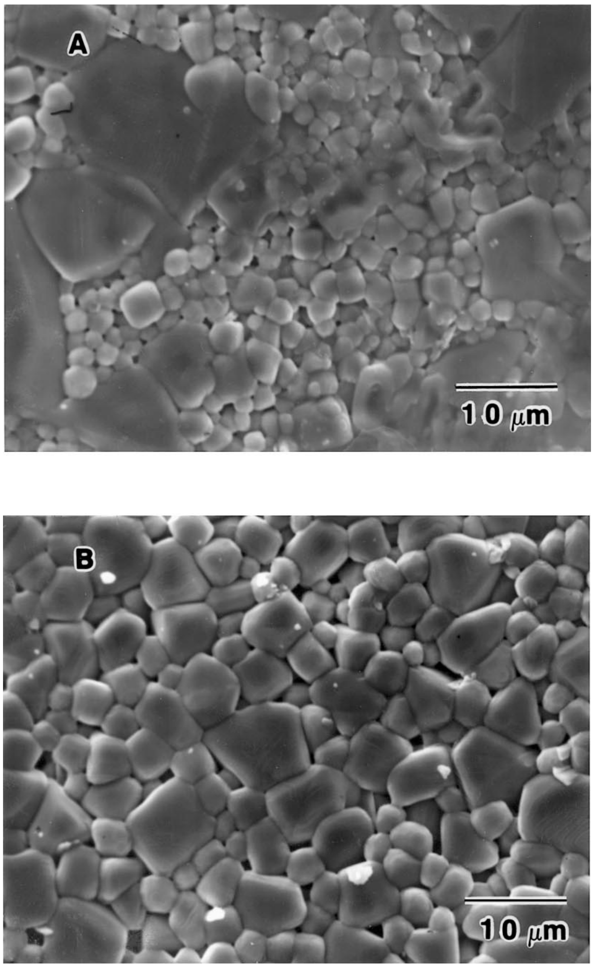

Figure 8 As sintered surface of Ba-excess $BaTiO_3$ with addition of SiO_2. (A) 0.5 mol % and (B) 2 mol %.

in SiO_2 concentration range of 1–2 mol %. In this concentration range, the average grain size is in the range of 5–10 μm. SEM microscopy in Fig. 8 shows that the uniformity of grain growth was improved at a 2 mol % concentration while bimodel-grains appear in samples with <1 mol % SiO_2, indicating the need for sufficient liquid phase to coat particles during the sintering. It was also found that grain growth increases to 30 μm as the SiO_2 concentration increases to 3 mol %. The results on electrical behavior as a function of SiO_2 concentration show that materials within the range of 0.25–0.5 mol % SiO_2 have a high interior resistivity (10^3–10^5 Ω·cm) through impedance analysis. Hence, optimum selection of SiO_2 to Ba-excess $BaTiO_3$ materials is around 2 mol % for obtaining optimum density and grain size as well as ρ_{RT}. For SiO_2 concentration over 1 mol %, a diffuse PTCR behavior of 2 orders is obtained with low ρ_{RT} (10^1–10^2 Ω·cm).

The electrical properties of higher Ba-excess ($Ba/Ti > 1.006$) $BaTiO_3$ was also investigated for a constant donor doping (Y_2O_3: 0.3 mol %) and SiO_2 content (2 mol %). It was found that ρ_{RT} in these materials increases to 10^3–10^6 Ω·cm without any improvement in PTCR rise. Minor adjustments to these parameters did not significantly improve results and it is, therefore, indicated that small Ba-excess rates ($Ba/Ti = 1.006$) produce optimum behavior.

Although Ba-excess $BaTiO_3$ materials show high density and low ρ_{RT}, the PTCR rise is only 2 orders magnitude as shown in Fig. 6. Small amounts of MnO (0.01–0.07 mol %) were added to these materials to promote PTCR behavior. Mn ions segregate near grain boundary regions to enhance the potential barrier [26]. Fig. 9 shows the enhanced properties of Ba-excess materials using a sintering temperature of 1330 °C with an annealing schedule of 1220 °C/10 h.

3.3. Domain microstructure in modified Ba-excess $BaTiO_3$

Domain microstructure observation in this study were used to analyze the interior resistivity-structure relationship. Fig. 10 shows the typical domain configuration as a function of Ba/Ti ratio and SiO_2 concentration. Fig. 10A shows a completely random domain structure ($Ba/Ti = 1.006$), where many domain sets are randomly

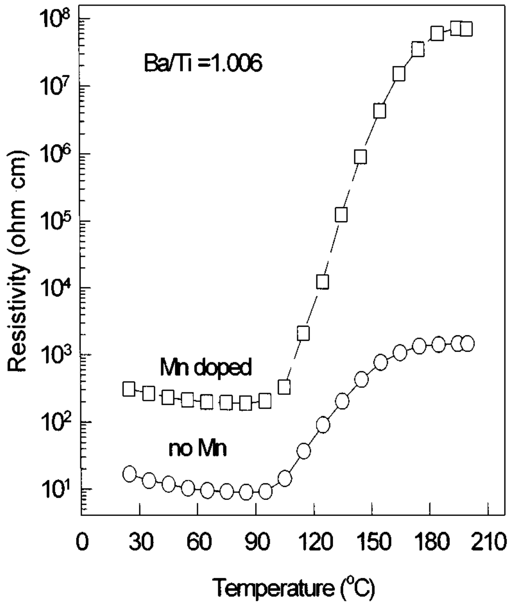

Figure 9 PTCR effect for Ba-excess materials with and without the presence of acceptor dopant MnO.

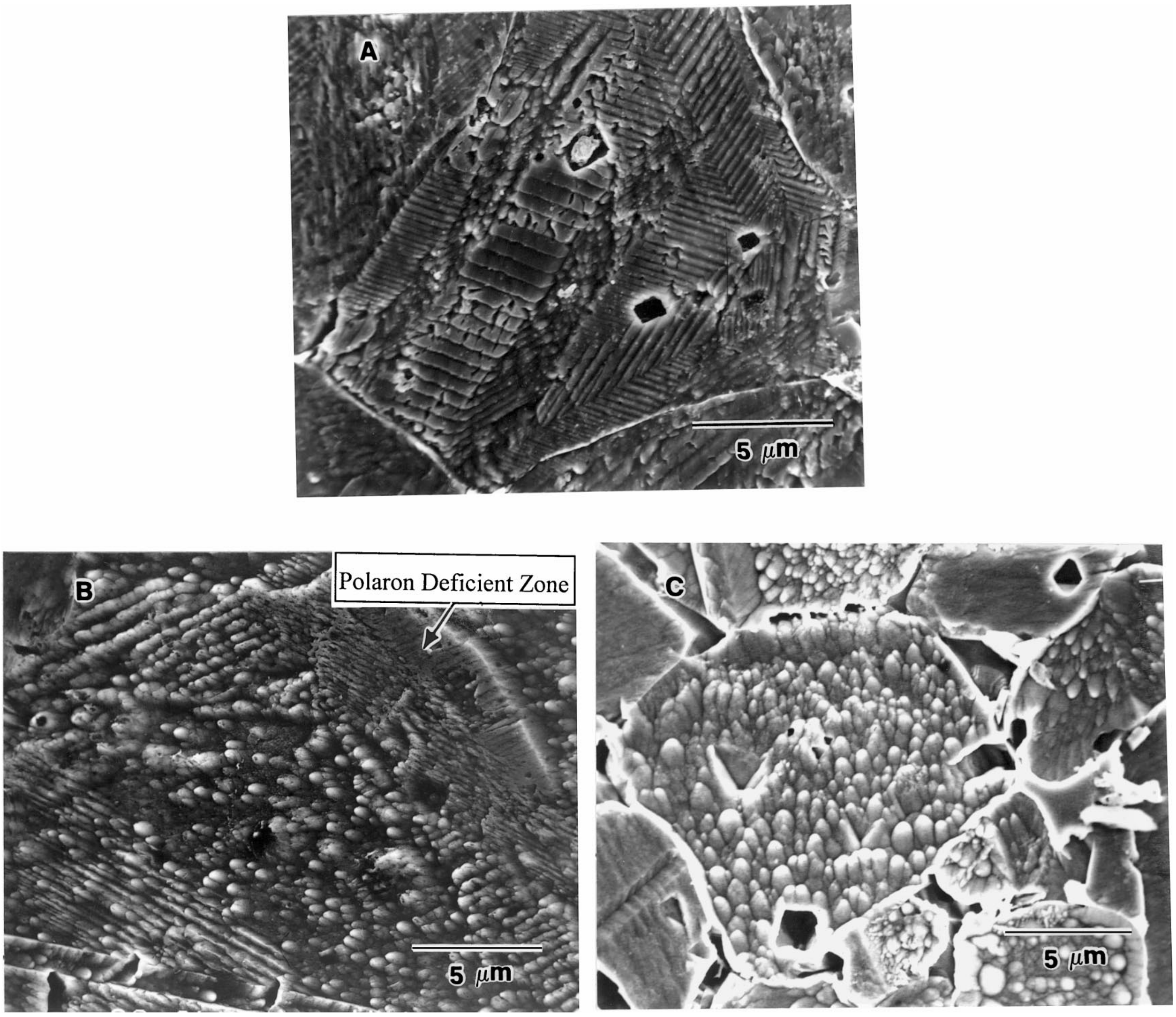

Figure 10 Domain structure development in donor doped Ba-excess $BaTiO_3$ with different SiO_2 concentration. (A) 0% (B) 0.5 mol % (C) 2 mol %.

oriented in a complex fashion within each individual grain. As a small amount of SiO_2 (0.25–0.5 mol%) is introduced, less random patterns are developed as shown in Fig. 10B. A completely uniform directional domain pattern across each grain in Ba-excess $BaTiO_3$ was obtained after more SiO_2 is added (>1 mol%), as shown in Fig. 10C. The domain alignment has previously been found to have a remarkable correspondence to the electrical resistivity [18, 22, 25].

Domain nucleation serves to relieve stress during the phase transformation near T_c. The driving force for directional nucleation is derived from the strong interaction between sufficient amounts of polaron formation, spontaneous polarization and local strain fields [18, 22, 25]. In directional domain structures, long domain columns pass through the entire grain with 90° domain boundaries. The electron transportation mechanism has high mobility along the pathway in each domain column parallel to 90° domain boundaries. The homogeneous directional domain structure appears in Ba-excess $BaTiO_3$ when sufficient liquid phase is present during sintering, where the donor is well dispersed, as shown in Fig. 10C. In the situation of poor donor dispersion, which exists in materials without enough liquid phase present, as shown in Fig. 10B, the result shows an absence of well-defined domain structure in some local area. These areas can be defined as "polaron deficient zones". In these zones, inhomogeneous dopant dispersion occurs and, therefore, the interaction between the polaron, surrounding strain field, and neighbor spontaneous polarization is minimized, creating non-uniformity within domain alignment. The mobility is decreased in these zones. From the viewpoint of microstructure, uniform directional domain alignment is desirable to pursue low ρ_{RT}, which requires sufficient liquid presence for dopant dispersion.

4. Conclusion

A narrow range of stoichiometry (Ba/Ti $=$ 0.997–1.006) was used to study the electrical response and microstructure in donor and acceptor modified $BaTiO_3$ as well as liquid phase sintering by adding SiO_2.

Expected Ba-excess behavior in the materials studied was found with a Ba/Ti ratio $\geq$ 1.006. Introduction of SiO_2 to Ba-excess materials can switch material from electrical insulator to semiconductor. It was found that SiO_2 influence the defect chemistry by dispersing donor at lower sintering temperature. The optimum SiO_2 concentration to adjust material grain growth and densifcation is approximately 2 mol %, corresponding to a proper Ba/Ti ratio 1.006. MnO was required to enhance PTCR response.

Directional alignment of the domain structure through each grain is indicative of a well-dispersed donor dopant in $BaTiO_3$. Conversion from random to a directional domain structure accompanies the transition from high resistance/dielectric behavior to low resistance PTCR behavior. "Polaron deficient zones" exist in Ba-excess materials with small amount of liquid phase present.

Acknowledgements

We thank Professor R. C. Buchanan for his generously supporting on the sample preparation and electrical measurements.

References

1. B. M. KULWICKI, "Advances in Ceramics," Vol. 1 (Amer. Ceram. Soc., 1980) p. 138.
2. S. HUYBRECHTS, K. ISHIZAKI and M. TAKATA, *J. Mater. Sci.* **30** (1995) 2463.
3. J. G. FAGAN and V. R. W. AMARKOON, *Amer. Ceram. Soc. Bulletin* **72** (1993) 69.
4. H. IHRIG, "Advance in Ceramics," Vol. 7 (Amer. Ceram. Soc., 1983) p. 117.
5. TSAI-FA LIN and CHEN-TI HU, *J. Amer. Ceram. Soc.* **73** (1990) 531.
6. G. ARLIT and U. ROBELS, *J. Appl. Phys.* **73** (1993) 3454.
7. H. B. HAANSTRA and H. IHRIG, *J. Amer. Ceram. Soc.* **63** (1980) 288.
8. K. R. UDAYAKUMAR, K. G. BROOKS and V. R. W. AMARAKOON, *Ceram. Eng. Sci. Proc.* **8** (1987) 1035.
9. H. M. AL-ALLAK, T. V. PARRY, G. J. RUSSELL and J. WOODS, *J. Mater. Sci.* **23** (1988) 1083.
10. H. UEOKA and M. YODOGAWA, *IEEE. Trans. Mfg. Tech.* **MFT-3** (1974) 77.
11. W. HEYWANG, *J. Mater. Sci.* **6** (1971) 1214.
12. W. HEYWANG, *Solid State Electronics* **3** (1961) 51.
13. G. H. JONKER, *ibid.* **7** (1964) 895.
14. G. H. JONKER, "*Advance in Ceramics*," Vol. 1 (Amer. Ceram. Soc., 1980) p. 155.
15. J. DANIELS, K. H. HAERDTL and R. WERNICKE, *Philip Tech. Res.* **38** (1979) 73.
16. B. M. KULWICKI and A. J. PURDES, *Ferroelectrics* **1** (1970) 253.
17. R. C. BUCHANAN, T. R. ARMSTRONG and R. D. ROSEMAN, *Ferroelectrics* **135** (1992) 343.
18. R. D. ROSEMAN, J. KIM and R. C. BUCHANAN, *ibid.* **177** (1996) 273.
19. M. KUWABAWA, "Advances in Ceramics," Vol. 17 (Amer. Ceram. Soc., 1981) 137.
20. G. V. LEWIS and C. R. A. CATLOW, *J. Amer. Ceram. Soc.* **68** (1985) 555.
21. *Idem., Br. Ceram. Pro.* **36** (1985) 187.
22. H. KONDOU, M. FUJIMOTO and S. SHEIRSAKI, *Jpn. J. Appl. Phys.* **28** (1989) 52.
23. M. P. HARMER, Y. H. HU, M. LAL and D. M. SMYTH, *J. Amer. Ceram. Soc.* **49** (1983) 71.
24. D. E. RASE and R. ROY, *ibid.* **38** (1955) 102.
25. P. V. LAMBECK and G. H. JONKER, *ibid.* **22** (1980) 729.
26. DA YU WANG and KAZUMASA UMEYA, *ibid.* **73** (1990) 669.
27. Y. H. HU, H. M. CHAN, Z. X. WEN and M. P. HARMER, *J. Amer. Ceram. Soc.* **69** (1985) 594.
28. Y. H. HU, M. P. HARMER and D. M. SMYTH, *ibid.* **68** (1985) 372.

Received 22 September 1998
and accepted 11 February 1999